Macromolecules

pubs.acs.org/Macromolecules Article

Exploiting Ion-Pairing Interactions for Fast and Controlled Ring-Opening Polymerization of *rac*-β-Butyrolactone at Room Temperature with Dinuclear Sodium and Potassium Catalysts

Changjuan Chen, Aijiang Zhang,* Chunshan Zuo, Jianghong Dong, Mingjian Ma, Shihao Zhang, Huyuan Guo, and Jing Fu

Cite This: *Macromolecules* 2024, 57, 9275−9288 Read Online

ACCESS | Metrics & More | Article Recommendations | Supporting Information

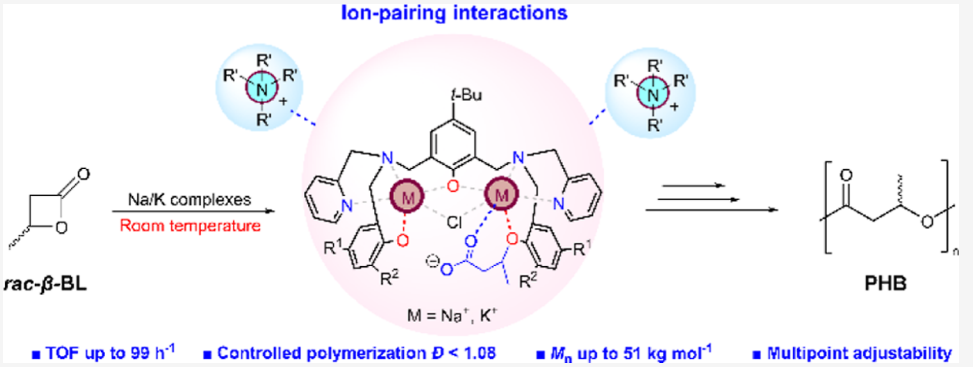

ABSTRACT: Poly(β-hydroxybutyrate) (PHB) is one of the best candidates as a sustainable plastic material for a circular economy due to its biorenewability, biodegradability, and biocompatibility. Compared with other metal catalysts that have made great progress, the highly active and controlled polymerization of *rac*-β-hydroxybutyrate (*rac*-BBL) for the synthesis of PHB using sodium and potassium catalysts at room temperature is still rarely reported and remains a great challenge. In this contribution, a series of novel and adjustable dinuclear sodium and potassium ion-pair catalysts were designed and synthesized, in which the optimized catalyst **2** allows for fast ring-opening polymerization (ROP) of *rac*-BBL (turnover frequency up to 99 h^{-1}) in bulk at room temperature to prepare PHB with predictable molar mass and excellent molecular weight distribution ($Đ$ = 1.06). The effect of the structure of catalysts such as the type of alkali metal ion, the electronic and steric effect of substituent groups, and the size of countercation on the ROP activity was systematically investigated. Single crystal X-ray diffraction, NMR, MALDI-TOF, and DTF calculations were utilized to uncover that the presence of the ion-pairing interactions within sodium- and potassium-based catalysts is considered to be crucial for both enhancing the nucleophilicity and reducing the alkalinity of the initiator (phenolate anion)/chain-end (carboxylate anion) during catalysis, thus effectively promoting polymerization reaction and suppressing adverse side reaction (e.g., deprotonation, base-promoted elimination, and chain scission) for gaining PHB with molecular weight (M_n) up to 51 kg mol^{-1}. This study provides fruitful information to deeply understand the catalytic role of ion-pairing interactions within sodium- and potassium-based catalysts, which would contribute to the design of novel, efficient, and eco-friendly catalysts for the polymerization of the other cyclic esters.

INTRODUCTION

The unparalleled surge of production, consumption, and indiscriminate disposal of petrochemical polymers and the slow environmental degradation of these polymers contribute to one of the greatest serious environmental problems in recent years.[1,2] This drives people who are eager to find sustainable polymer alternatives that can be decomposed in soil and marine environments without harming the organisms.[3−5] Among sustainable polymers, poly(β-hydroxybutyrate) (PHB) is one of the most promising alternatives to petrochemical polymers because of good biodegradability, general biocompatibility, and wide applications in daily life and medicine.[6,7] However, large-scale production of PHB employing expensive biological routes has seriously restricted the speed of its promotion as commodity materials.[8,9] Consequently, the development of simple, fast, and efficient

Received: August 27, 2024
Revised: September 4, 2024
Accepted: September 10, 2024
Published: September 24, 2024

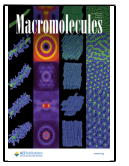

https://doi.org/10.1021/acs.macromol.4c02043
Macromolecules 2024, 57, 9275−9288

Scheme 1. Synthesis Route of the Dinuclear Alkali Metal Ion-Pair Complexes 1 and 2 with H_3L_1

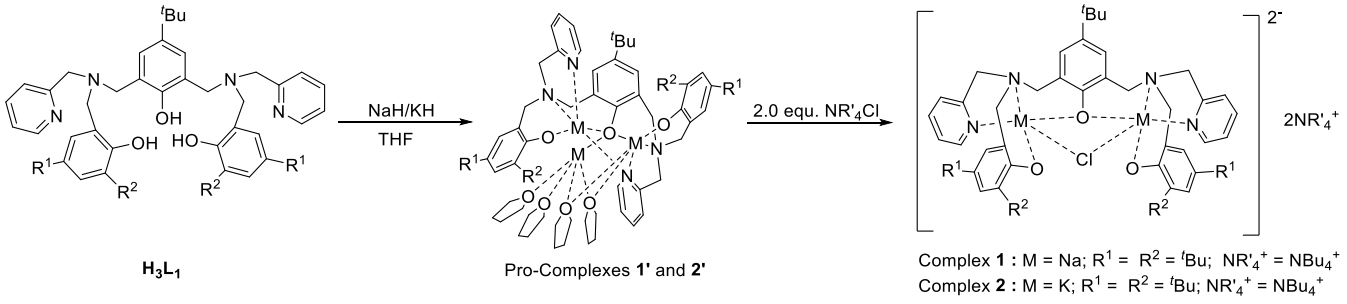

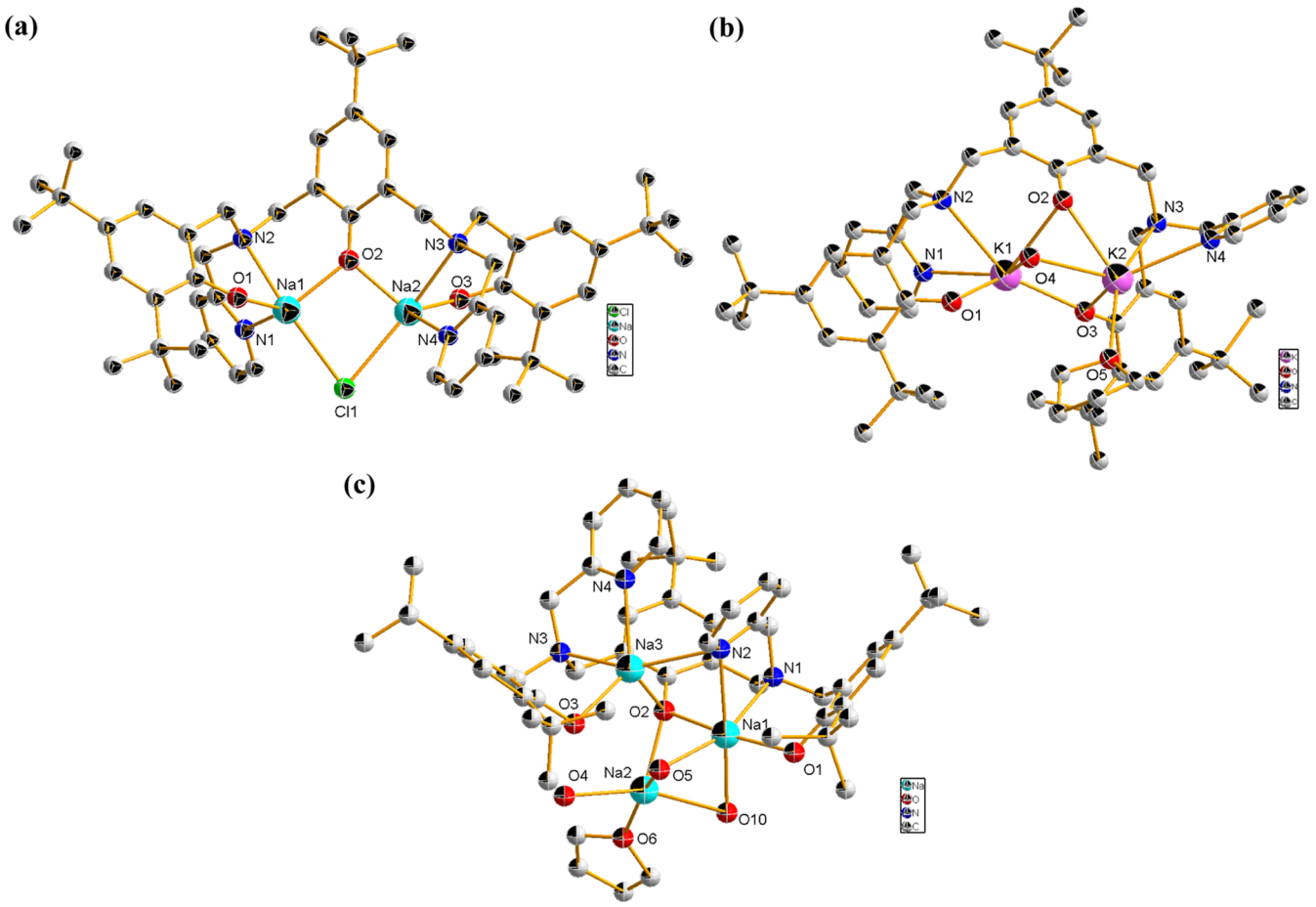

Figure 1. Crystal structures of complex **1** (a), complex **2″** (b), and pro-complex **1′** (c). All hydrogen atoms and tetrabutylammonium cations were omitted for clarity, and the thermal ellipsoids were drawn at the 50% probability level.

chemical methods to prepare PHB by adopting appropriate catalysts would be a desirable alternative.[10−12] One of the most straightforward and effective chemical methods to access PHB is the ring-opening polymerization (ROP) of *β*-hydroxybutyrate (BBL) catalyzed by all kinds of metal-based catalysts including rare earth,[13−19] chromium,[20,21] zirconium,[22,23] zinc,[8,24−26] aluminum,[27,28] indium,[29−31] and tin,[32] which possess high activity and remarkable ability to control precisely the architectures such as molar mass, dispersity, and tacticity. Nevertheless, these metal residues in PHB are often colored, toxic, and difficult to remove, leading to contamination of the resultant polymer and impeding its applications in the food packing, biomedical, and microelectronic fields.[33,34]

From the aspects of green chemistry and sustainable development,[35−37] the exploitation of abundant, nontoxic, biocompatible, and cheap metal catalysts such as sodium and potassium for the catalytic synthesis of PHB is highly desirable. However, the ROP of BBL is particularly difficult because the active intermediate is prone to deactivation, and some side reactions[38,39] such as backbiting reaction, transesterification, deprotonation, elimination, and chain scission frequently occur during its polymerization. Generally, the common sodium and potassium alkoxides or carboxylates could not induce polymerization of BBL at room temperature.[40] The introduction of crown ethers or cryptands in these sodium and potassium alkoxides or carboxylates and the choice of a highly polar aprotic solvent such as dimethyl sulfoxide (DMSO) for weakening the strong ion-pairing interactions are two common general strategies to improve the nucleophilicity of corresponding anions and obtain better catalytic activity.[41,42] These

https://doi.org/10.1021/acs.macromol.4c02043
Macromolecules 2024, 57, 9275−9288

Table 1. *rac*-BBL Polymerization Catalyzed by Complexes 1−7 and 2′

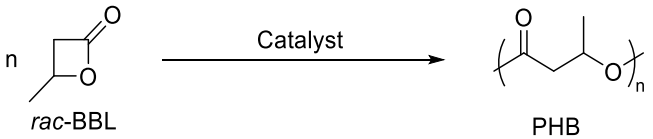

rac-BBL PHB

entry[a]	cat.	[*rac*-BBL]$_0$/[cat.]$_0$	temp. (°C)	time[b] (h)	conv.[c] (%)	TOF[d] (h^{-1})	$M_{n,obsd}$.[e] (g/mol)	$M_{n,calcd}$.[f] (g/mol)	Đ
1	**1**	200:1	r.t.	2	68	68	5700	5900	1.05
2	**2**	200:1	r.t.	2	92	92	7600	7900	1.05
3	**2**	100:1	r.t.	1	99	99	4100	4300	1.06
4	**2**	400:1	r.t.	4	90	90	15,200	15,500	1.03
5	**2**	800:1	r.t.	9	95	84	32,500	32,700	1.04
6	**2**	1200:1	r.t.	13	92	85	47,000	47,500	1.04
7	**2**	1600:1	r.t.	20	90	72	51,100	62,000	1.06
8	**2**	2000:1	r.t.	32	92	58	49,500	79,200	1.05
9	**2′**	200:1	r.t.	2	8	8	n.d.	n.d.	n.d.
10[g]	**2**	200:1	r.t.	2	52	52	4200	4500	1.04
11[h]	**2**	200:1	r.t.	2	45	45	3600	3900	1.04
12	**2**	200:1	60	30 min	94	376	6200	8100	1.12
13	**2**	200:1	100	12 min	97	970	5600	8400	1.28
14	**3**	200:1	r.t.	2	87	87	7300	7500	1.05
15	**4**	200:1	r.t.	2	60	60	4900	5200	1.05
16	**5**	200:1	r.t.	2	78	78	6600	6700	1.04
17	**6**	200:1	r.t.	2	48	48	3900	4100	1.06
18	**7**	200:1	r.t.	2	21	21	1500	1800	1.08

[a]All polymerizations were performed in bulk except entries 10 (THF) and 11 (toluene), [*rac*-BBL] = 5.0 M. [b]No optimized reaction time. [c]The conversion was determined by ^{1}H NMR spectra integration of methyne resonances of BBL and PHB. [d]Turnover frequency (TOF) was calculated with the relation: (mol *rac*-BBL consumed) × catalyst^{-1}× h^{-1}. [e]Experimental M_n and Đ determined by GPC calibrated with polystyrene standards in THF at 40 °C. [f]Calculated from the relation: [BBL]$_0$/(2 × [cat.]$_0$) × conversion × M_{BBL} with M_{BBL} = 86.09 g/mol. [g]Polymerization was performed in THF. [h]Polymerization was performed in toluene. n.d., not determined.

strategies indeed can improve reaction activities, but they still take a long reaction time for several days or even weeks at room temperature [turnover frequency (TOF) < 2.25 h^{-1}] in bulk.[43] The low efficiency and the limited adjustability of these current catalytic systems containing sodium and potassium obviously cannot satisfy people's growing needs for biodegradable PHB. Therefore, the exploitation of highly active sodium and potassium catalytic systems is a meaningful yet challenging job.

Inspired by the abovementioned research work, we recognized that ion-pairing interactions may be a key factor that can influence the catalytic activities of sodium- and potassium-based catalysts in the ROP of BBL. In fact, ion-pairing interactions originated from electrostatic attraction between two groups of opposite charge as a powerful strategy for increasing reactivity and controlling reaction selectivity in chemical reactions have attracted intensive attention because these interactions play a decisive role in the outcome of reactions that involve charged reagents, intermediates, or catalysts.[44−53] Based on the abovementioned considerations, we envisioned synthesizing dinuclear sodium and potassium ion-pair complexes that wish to effectively and controllably catalyze the ROP of *rac*-BBL for producing biodegradable PHB. The ion-pairing interactions between the anion and cation of these complexes can be easily regulated by changing the size of the countercations, the steric hindrance and electronic effect of substituents, and the type of metal centers. Meanwhile, the effects of these ion-pairing interactions on the polymerization behavior for the ROP of BBL will be systematically investigated by density functional theory (DFT) theoretical calculation and control experiment. We expect that this study will help to understand the role of ion-pairing interactions in polymerization reactions and provide new ideas for the design and synthesis of the next generation of efficient and environmentally friendly catalysts.

RESULTS AND DISCUSSION

Design and Synthesis of Dinuclear Sodium and Potassium Ion-Pair Complexes. To obtain dinuclear sodium and potassium ion-pair complexes, we have designed and synthesized a multidentate ligand H_3L_1 containing three acidic phenolic hydroxyl groups and only two N_2O_2 metal-chelating sites. It could be easily prepared via a sequence of well-studied high-yield Schiff base condensation/reduction/nucleophilic substitution reactions using simple and readily available reagents (Schemes S1 and S2 and Figures S1 and S2). Subsequently, H_3L_1 continuously reacted with NaH/KH and tetrabutyl ammonium chloride to gain complexes **1** and **2** (Schemes 1 and S3, Figures S3−S10).

Initially, we imagined that the reaction of (1 equiv) H_3L_1 with (3 equiv) NaH/KH deprotonated three hydrogen atoms to form a trinuclear sodium or potassium complex. Because it possesses only two chelating centers in H_3L_1, one metal ion exposed to the outside would be easily replaced by one $N^nBu_4^+$ cation to form a dinuclear ion-pair complex in which the ratio of L_1^{3-} and $N^nBu_4^+$ cation is 1:1. Interestingly when examining the ^{1}H NMR spectra of complexes **1** and **2**, we found that the ratio of the L_1^{3-} and $N^nBu_4^+$ cation is 1:2 (Figures S7 and S9). To explain the discrepancy between expectations and reality, we attempted to crystallize **1** and **2** for X-ray structural validation. Fortunately, crystals of **1** and **2″** (the partial hydrolysis product of **2**) suitable for diffraction data collection

https://doi.org/10.1021/acs.macromol.4c02043
Macromolecules 2024, 57, 9275−9288

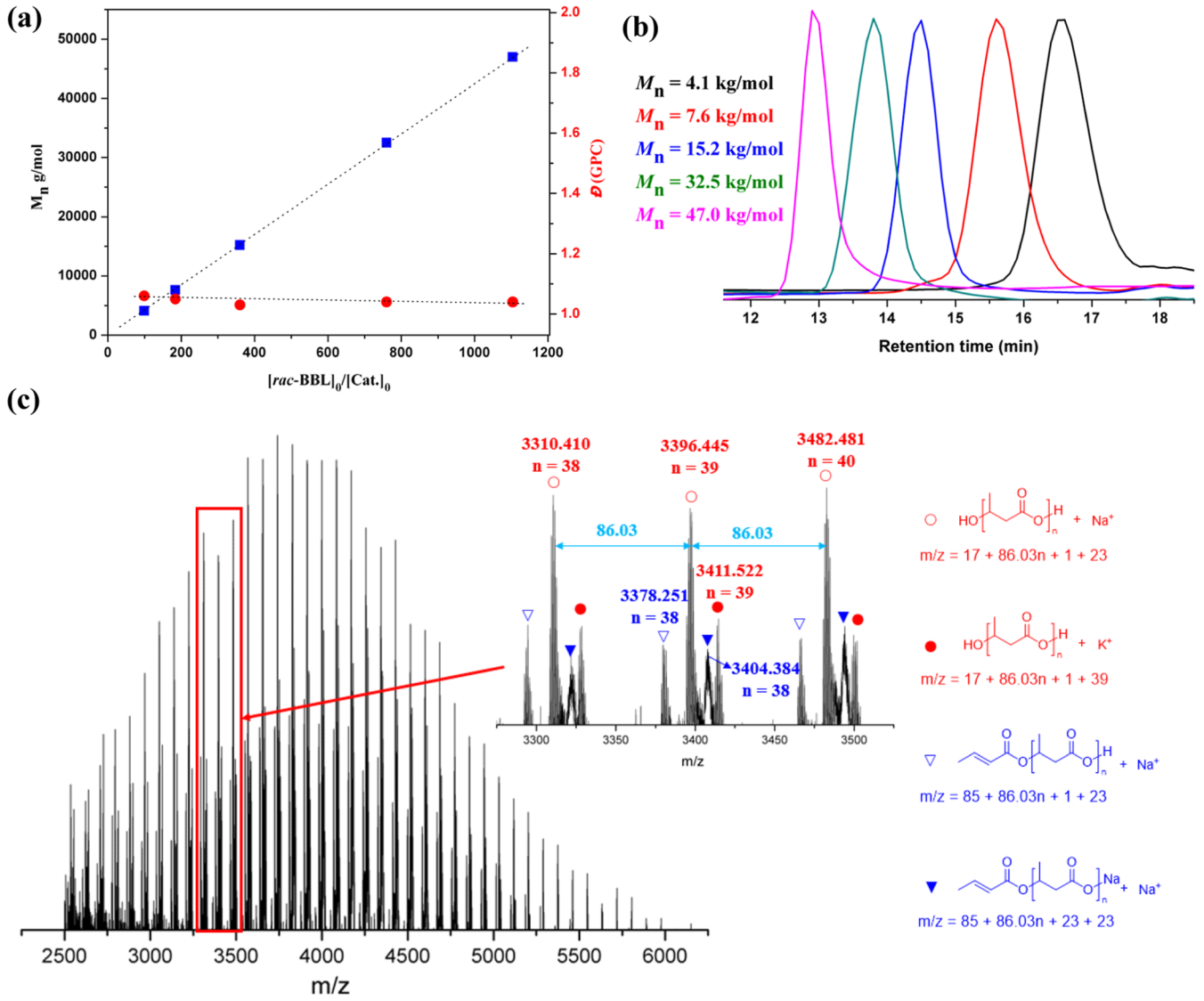

Figure 2. (a) Plots of the relationship between M_n (■) and $Đ$ (●) of the polymer catalyzed by complex **2** and the initial mole ratio [*rac*-BBL]$_0$/[cat.]$_0$ (Table 1, entries 2–6). (b) Representative gel permeation chromatography (GPC) traces of the PHB prepared by complex **2** (Table 1, entries 2–6). (c) MALDI-TOF mass spectrum (matrix: DHB; ionization salt: CF_3CO_2Na; solvent: THF) of the PHB sample synthesized by complex **2** (Table 1, entry 3). Na^+ could come from the CF_3CO_2Na, and K^+ could come from complex **2**.

were obtained from a mixture solution of tetrahydrofuran and *n*-hexane (Table S1).

X-ray crystallographic analysis displayed that **1** indeed forms a bimetallic structure that contains a $[Na_2(\mu_2\text{-}L_1)(\mu_2\text{-}Cl)]^{2-}$ anion by a bridging phenolate and a bridging chloride ion (Figure 1a). The presence of a bridging chloride ion in **1** led to two positive $N^nBu_4^+$ counterions on the periphery of the $[Na_2(\mu_2\text{-}L_1)(\mu_2\text{-}Cl)]^{2-}$ unit, being consistent with the result of the ^{1}H NMR spectrum (Figure S7). The two pentacoordinate sodium atoms have similar distorted trigonal bipyramidal coordination environment (τ_1 = 0.67 for Na1, τ_2 = 0.70 for Na2, the value of τ ranges from 1.00 for a perfect trigonal bipyramidal geometry to 0 for an ideal square pyramidal geometry[S4]), each coordinated to one pyridyl and one tertiary amine nitrogen atom, two phenolate oxygen atoms, and one chloride ion. Due to the high activity and hygroscopicity of **2**, the partial hydrolysis product complex **2″** was always obtained during crystallization. The crystal structure of **2″** revealed that the dinuclear nature of this complex is like that of **1**, where the two K^+ ions are bridged by two O atoms of different phenolate anions and one O atom of water (Figure 1b), and the ratio of L_1^{3-} and $N^nBu_4^+$ cation is 1:1. However, the ^{1}H NMR spectrum of **2** showed that the ratio of L_1^{3-} and $N^nBu_4^+$ cation is 1:2, implying that the bridging chloride ion could be replaced by one water molecule and released from **2** in the form of tetrabutylammonium chloride. Based on the NMR spectra of **1** and **2** combined with the crystal structure of **1** and **2″**, we reasoned that **2** has a similar structure to **1**. Fortunately, we also obtained crystals of procomplex **1′** using the same method as **1**. As might be expected, the crystal structure shows that **1′** is trinuclear in the solid state with the three sodium ions, of which two sodium ions (Na1 and Na3) are in the chelating center (N_2O_2 or N_3O_2) of L_1^{3-} and one exposed sodium ion (Na2) is coordinated to only one oxygen atom of the phenoxy group of L_1^{3-} and to four oxygen atoms of water or THF molecules. These water molecules in crystal **1′** might originate from the moisture in the air during the process of growing the crystals (Figure 1c, Table S1).

https://doi.org/10.1021/acs.macromol.4c02043
Macromolecules 2024, 57, 9275−9288

Catalytic Performance and End-Group Characterization. The above sodium and potassium ion-pair complexes **1** and **2** were used to evaluate their catalytic performance for the ROP of *rac*-BBL. Surprisingly, the conversions of *rac*-BBL could reach 68% (TOF = 68 h^{-1}) and 92% (TOF = 92 h^{-1}) for **1** and **2**, respectively, within 2 h at room temperature in bulk with a 200:1 ratio of $[rac\text{-BBL}]_0/[\text{cat.}]_0$, producing the PHBs with narrow molecular weight distribution ($Đ$ = 1.05, Table 1, entries 1−2). Since the experimental molecular weights (M_ns) seemed consistent with two polymer chains growing simultaneously per **2**, the calculated M_ns were calculated by assuming that two polymer chains propagate per **2**. With the above encouraging results, the controlled property of the more active **2**-mediated ROP was further investigated by changing the molar ratio of the monomer to the catalyst in the bulk at room temperature. When the ratio of $[rac\text{-BBL}]_0/[\mathbf{2}]_0$ was increased from 100:1 to 1200:1, the molecular weights of resultant polymers agreed well with calculated values and increased linearly with the ratios of $[rac\text{-BBL}]_0$ to $[\mathbf{2}]_0$ (Table 1, entries 2−6, and Figure 2a), and the molecular weight distributions also were very narrow (1.03−1.06). In addition, the corresponding gel permeation chromatography (GPC) traces clearly showcased five unimodal peaks and exhibited an increasing evolution of M_n (Figure 2b). Such results showed that the **2**-mediated polymerization of *rac*-BBL indicates a controlled characteristic. Nevertheless, when the ratio of $[rac\text{-BBL}]_0$ to $[\mathbf{2}]_0$ was increased to 1600:1 and 2000:1 (Table 1, entries 7 and 8), the polymerization deviated from an ideal living behavior despite high molecular-weight PHBs being produced (the highest molecular weight PHB is up to 51 kg mol^{-1}).

Subsequently, the structure of resultant PHBs was investigated by ^{1}H NMR spectroscopy and matrix-assisted laser desorption/ionization time-of-flight (MALDI-TOF) mass spectrum. The ^{1}H NMR spectrum of low molecular weight PHB displayed that besides the four large characteristic peaks at 1.3 ppm (methyl), 2.5 and 2.6 ppm (methylene), and 5.2 ppm (methine) assignable to the main chain repeating butyrate units, small peaks of crotonate, −OH and −COOH were notable that could be attributed to the end-groups (Table 1, entry 3, and Figures S11 and S12). The MALDI-TOF mass spectrum provided more accurate information. As shown, four populations were exhibited, each of which repeats in intervals of 86.03, commensurate with one unit of BBL (Figure 2c). The two major populations (marked by red circle and dot) corresponded to the linear PHB with a hydroxy at one end and a carboxylate at the other end (expressed as $[OH + (C_4H_6O_2)_n + H + Na]^+$, $m/z = 17 + 86.03n + 1 + 23$ and $[OH + (C_4H_6O_2)_n + H + K]^+$, $m/z = 17 + 86.03n + 1 + 39$). The third distribution (marked by blue triangles) was derived from polyesters terminated by a crotonate group and a carboxylate group (expressed as $[C_4H_5O_2 + (C_4H_6O_2)_n + H + Na]^+$, $m/z = 85 + 86.03n + 1 + 23$). The fourth distribution (marked by solid triangles) was assigned to the third population counterpart, where H^+ was exchanged with Na^+ (expressed as $[C_4H_5O_2 + (C_4H_6O_2)_n + Na + Na]^+$, $m/z = 85 + 86.03n + 23 + 23$). These results indicated that **2** could catalyze by the ROP of *rac*-BBL for the synthesis of linear PHBs that mainly possess hydroxyl and carboxylate groups as chain ends.

Impact of the Ion-Pairing Interactions on Catalytic Activity. The above-mentioned experimental results indicated that **1** and **2** exhibited far higher activity over the ROP of *rac*-BBL compared to that of the reported crown ethers or cryptand/alkali-metal salts binary catalytic system as the catalysts (TOF < 2.25 h^{-1}).[43,55] To investigate whether the ion-pairing interactions play a key role in the improvement of catalytic activity in this catalytic system, we carried out the following control experiment using the neutral pro-complex **2′** instead of complex **2** as a catalyst for the ROP of *rac*-BBL under the identical condition ($[rac\text{-BBL}]_0/[\text{cat.}]_0$ = 200:1, bulk, 2 h, room temperature). As expected, a negligible conversion of 8% was observed (Table 1, entry 9). How exactly do ion-pairing interactions play a role in improving the catalytic activity in this system? To understand this problem, we performed a DFT calculation to determine the charge distribution of **2′** and **2**. The geometries of **2′** and **2** were optimized by using DFT calculation at the B3LYP 6-31G (d, p) level based on the crystal structures of **1′** and **1**. The results showed that the oxygens of the peripheral phenolate anion in **2** carry the negative charge of −0.735 and −0.724, respectively (see the computational details of Supporting Information). Confusingly, the oxygens of the peripheral phenolate anion in **2′** carry the negative charge of −0.769 and −0.728, which is more electronegative than that in **2**, signifying that **2′** seems to have a higher catalytic activity than **2** due to the greater nucleophilic capacity. These data that contradicted the experimental results made us realize that **2′** and **2** are complexes with different structures. The phenolate anion in **2′** combines with K^+ to form a neutral complex through a coordination bond. However, the phenolate anion in **2** binds to K^+ via the coordination bond to form the $[K_2(\mu_2\text{-}L_1)(\mu_2\text{-}Cl)]^{2-}$ anion, resulting in the presence of two $N^nBu_4^+$ in the periphery in order to conform with the principle of electric neutrality. Therefore, compared with **2′**, the nucleophilicity of the phenolate anion in **2** is affected not only by K^+ but also by the peripheral countercation.

To explore the influence of the peripheral countercation on the nucleophilicity of phenolate anion, the free energies of association of **2** and **2′** were calculated. The results of the calculation revealed that the free energy of association of **2′** is 8.8 kcal/mol larger than that of **2**, indicating that although the electronegativity of the phenolate anion in **2′** is stronger, the strong coordination interactions between the phenolate anion and K^+ will greatly weaken its nucleophilic ability. In other words, ion-pairing interactions between the $N^nBu_4^+$ cation and $[K_2(\mu_2\text{-}L_1)(\mu_2\text{-}Cl)]^{2-}$ anion in **2** will greatly offset the coordination interactions between K^+ and phenolate anion, making the phenolate anion more free and more nucleophilic. As a result, **2** showed higher catalytic activity in the ROP of *rac*-BBL under the same reaction conditions compared to pro-complex **2′**. The above experiments and calculation results demonstrated that ion-pairing interactions play a crucial role in promoting the catalytic activity of the ROP of *rac*-BBL in these sodium- and potassium-based catalysts.

Effect of Solvent, Temperature, and Catalyst Structure on Catalytic Activity. To deeply understand the relationship between structure and activity, the influences of solvent, temperature, and the structure of sodium and potassium ion-pair complexes on the ROP of *rac*-BBL were comprehensively investigated, and the results are shown in Table 1. It is well-known that the polarity of the solvent usually affects the catalytic activity of the ion-pair catalyst. The ROP of *rac*-BBL was carried out by using the more active **2** in different solvents, and we found that the catalytic activity in THF was higher than that in toluene. For instance, when THF and toluene were used as solvents, the conversions of *rac*-BBL at

https://doi.org/10.1021/acs.macromol.4c02043
Macromolecules 2024, 57, 9275−9288

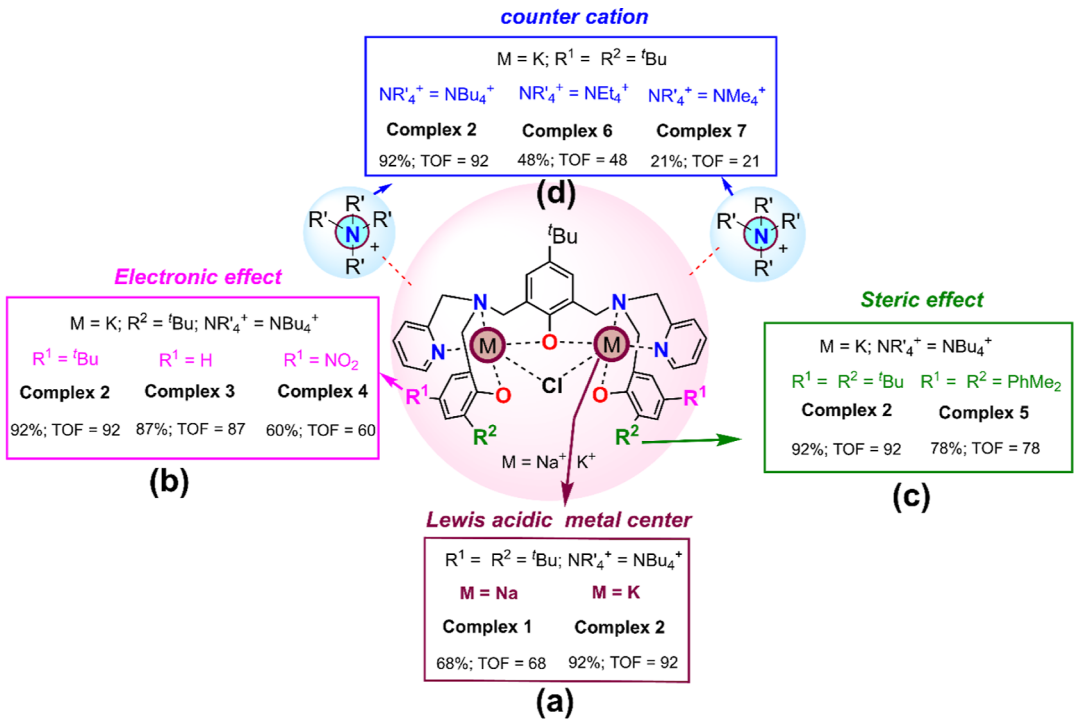

Figure 3. Systematic study on structure−activity relationships of dinuclear sodium and potassium ion-pair complexes as catalysts. The conversions were determined by ^{1}H NMR spectra integration of methyne resonances of *rac*-BBL and PHB. The TOF values of these catalysts were determined at room temperature in bulk for 2 h with $[rac\text{-BBL}]_0/[\text{cat.}]_0$ = 200:1.

room temperature after 2 h were 52% and 45%, respectively (Table 1, entries 10 and 11). We speculated that the polar THF could effectively weaken the ion-pairing interactions between the cation and anion in **2**, compared to the nonpolar toluene, making the phenolate anion more nucleophilic and active. To verify this, we calculated the free energy of association of **2** in THF and toluene, respectively, and found a relatively larger value in toluene than that in THF (−329.7 vs −194.2 kcal/mol), indicating that using THF as a solvent is more favored.

Due to the green economy of bulk reaction, we chose bulk reaction to study the influence of temperature on the ROP of *rac*-BBL by **2**. When the reaction temperature was increased to 60 °C, the conversion could reach 94% in 30 min with a 200:1 ratio of $[rac\text{-BBL}]_0/[\mathbf{2}]_0$ (Table 1, entry 12). Further increasing the temperature to 100 °C, the conversion could be increased to 97% in 12 min (Table 1, entry 13). These results illuminated that the catalytic activity increased obviously with increasing polymerization temperature; on the other hand, with the temperature rising, the controllability of the polymerization reaction became worse due to more side reactions, leading to broader dispersity (Table 1, entries 12 and 13, $Đ$ = 1.12 and 1.28) and bigger deviation between the experimental M_ns and predicted theoretically M_ns. Therefore, the effect of the catalyst structure on the ROP of *rac*-BBL was investigated at room temperature in bulk for 2 h with $[rac\text{-BBL}]_0/[\text{cat.}]_0$ = 200:1 as a benchmark condition.

The structures of all catalysts were well-defined by ^{1}H and ^{13}C NMR spectra (Schemes S1−S3, and Figures S13−S28). First, the effect of the type of alkali metal ion on catalytic activity was discussed. Compared with **2** (TOF = 92 h^{-1}) containing K^+ with the ionic radius of 1.38 Å, **1** bearing more smaller ionic radius (Na^+ = 1.02 Å) showed retarded reactivity with a TOF value of 68 h^{-1} (Table 1, entries 1 and 2; Figure 3a). This reduction of the reactivity can be attributed to the strengthened coordination interactions between Na^+ with a smaller ionic radius and phenolate anion, enabling the nucleophilicity of the phenolate anion to decline in **1**. Second, we investigated the electronic effect of substituent groups of **2**, **3**, and **4** on the catalytic activity of *rac*-BBL. When the substituent of the phenoxide unit at the R^2 position was fixed as a ^{t}Bu group, the activity of catalysts with higher TOFs was observed in the order of **2** (R^1 = ^{t}Bu, 92 h^{-1}) > **3** (R^1 = H, 87 h^{-1}) > **4** (R^1 = NO_2, 60 h^{-1}) as the electron-withdrawing ability of the substituents of the phenoxide unit at the R^1 position increased (Table 1, entries 2, 14, and 15; Figure 3b). These results indicated that the electron-donating group at the R^1 position is favorable to the ROP of *rac*-BBL to synthesize PHB. This can be attributed to the fact that the electronegativity of the phenolate anion is enhanced by the introduction of electron-donating groups at its para position, and thus, the nucleophilicity of the phenolate anion is enhanced. By comparing the Mulliken charges of phenolate anions in **1** (−0.710, −0.700), **2** (−0.735, −0.724), **3** (−0.731, −0.719), and **4** (−0.701, −0.644), which bear the same countercation ($N^nBu_4^+$), the calculated results agreed well with the experimental results that **2** is more active than **1**, and **2** is more active than **3** and **4**. In addition, the effect of **2** (R^1 = ^{t}Bu, R^2 = ^{t}Bu) and **5** (R^1 = Cumyl, R^2 = Cumyl) with different steric hindrances on the activity in the ROP of *rac*-BBL was also investigated. The activity of **5** with bulkier steric groups at the ortho position of the phenolate anion was lower than that of **2** under the same reaction conditions (Table 1, entries 2 and 16; Figure 3c).

Finally, a series of ion-pair potassium complexes **2** ($N^nBu_4^+$), **6** ($N^nEt_4^+$), and **7** ($N^nMe_4^+$) containing counterpart cations with different alkyl chain lengths on the catalytic activity of *rac*-BBL were studied. The results showed that the smaller

https://doi.org/10.1021/acs.macromol.4c02043
Macromolecules 2024, 57, 9275−9288

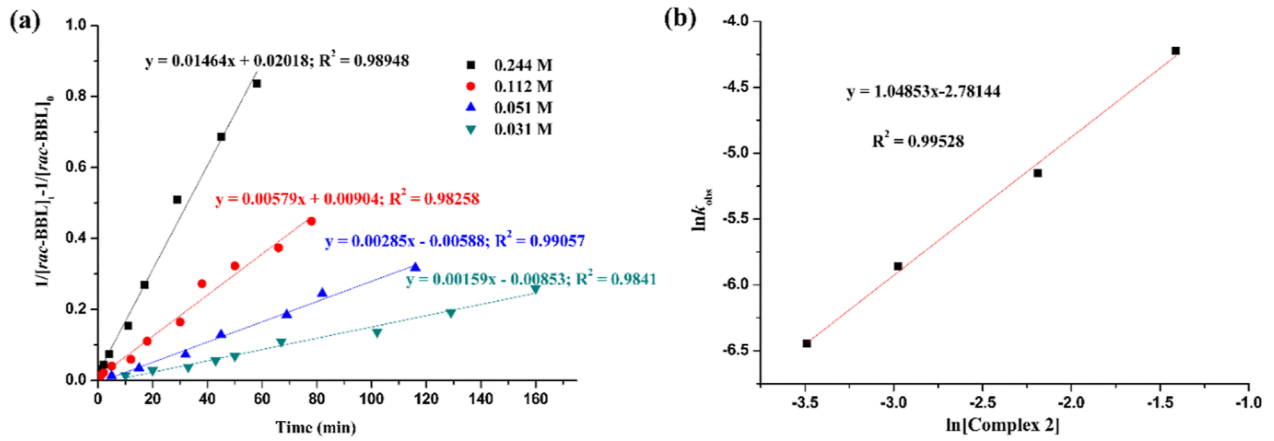

Figure 4. (a) Kinetic plots of $(1/[rac\text{-BBL}]_t - 1/[rac\text{-BBL}]_0)$ versus time for the polymerization of *rac*-BBL by complex **2** at 25 °C. $[\text{Complex } \mathbf{2}]_0$ = 0.244, 0.112, 0.051, and 0.031 M, $[rac\text{-BBL}]_0$ = 11.9 M. (b) Plots of ln k_{obs} versus ln[complex **2**]$_0$ for the polymerization of *rac*-BBL with complex **2** as a catalyst at 25 °C. $[rac\text{-BBL}]_0$ = 11.9 M.

Scheme 2. Two Potential Initiation Mechanisms for the ROP of (*S*)-BBL

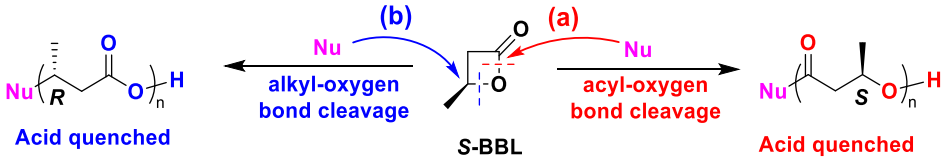

countercation reduce the reactivity of the ROP reaction. For example, when increasing the alkyl chain length of tetraalkylammonium from C1 to C4, the TOF value dramatically increased from 21 h^{-1} (by **7**) to 48 h^{-1} (by **6**) and 92 h^{-1} (by **2**) (Table 1, entries 2, 17 and 18; Figure 3d). By calculating the free energy of association between $[K_2(\mu_2\text{-}L_1)(\mu_2\text{-Cl})]^{2-}$ anions and $N^nR_4^+$cations of **2**, **6**, and **7** in toluene, it was found that the values of free energy of association of the three complexes are similar, which are presented in the order **7** (−91.0 kcal/mol) > **2** (−89.2 kcal/mol) > **6** (−87.6 kcal/mol). The present calculated results are not completely consistent with the experimental results. We speculated that other factors (e.g., the solubility of the catalyst) can also affect the catalytic activity besides the nucleophilicity of phenolate anion. In fact, we found that the solubility of these complexes becomes worse with the decrease of alkyl chain length of tetra-alkyl ammonium in the preparation process of these complexes. A similar behavior was reported using tetraalkylammonium carboxylate as organocatalysts for the ROP of *N*-carboxyanhydrides.[56] The above experimental results manifested that the type of alkali metal ion, the electronic effect and steric hindrance of substituent groups, and the size of the countercation in the ion-pair catalysts are of key importance in tuning the catalytic activity in the ROP of *rac*-BBL. All in all, any measures that can enhance the nucleophilicity of phenolate anion are conducive to enhancing the reactivity.

Kinetic Studies. To gather in-depth insight into the catalytic mechanism of dinuclear sodium and potassium ion-pair catalysts, the kinetic measurements of *rac*-BBL catalyzed by **2** were carried out in bulk at room temperature where initial *rac*-BBL concentration ($[rac\text{-BBL}]_0$ = 11.9 M) was held constant and catalyst concentration was varied from 0.031 to 0.244 M (Table S2). The ^{1}H NMR spectrum was applied to determine the conversion of *rac*-BBL. In all cases, plots of $(1/[rac\text{-BBL}]_t - 1/[rac\text{-BBL}]_0)$ vs time are linear, displaying polymerization proceeds with a second-order dependence on monomer concentration (Figure 4a). Therefore, the rate of the ROP can be written as $-d[rac\text{-BBL}]/dt = k_{obs}[rac\text{-BBL}]^2$, where $k_{obs} = k_p[\mathbf{2}]^n$, and k_p is the propagation constant. In addition, the observed rate coefficient (k_{obs}) can be acquired from the slope of the fitted regression line of Figure 4a. Because the equation of $k_{obs} = k_p[\mathbf{2}]^n$ can be described as ln k_{obs} = ln k_p + n × ln[**2**], plotting ln k_{obs} vs ln[**2**] allows us to determine n (the order in **2** concentration). A linear dependence was found between ln k_{obs} and ln[**2**] (Figure 4b), whose regression equation is expressed as ln k_{obs} = −2.78144 + 1.04853 × ln[**2**], suggesting that n equals 1.04853, that is, such polymerization catalysis is first-order in **2**. Therefore, the overall rate law can be proposed as $-d[rac\text{-BBL}]/dt = k_p[rac\text{-BBL}]^2[\mathbf{2}]^1$, where k_p is the propagation rate constant (k_p = 5.47 × 10^{-2} M^{-2} min^{-1}). The first-order dependence on **2** and second-order dependence on the *rac*-BBL concentration during the ROP process revealed that two peripheral phenolate anions of **2** independently initiate the monomer to generate respective polymer chains.

Initiation Mechanism Study and Computational Study on the 2-Mediated ROP Process. Coming from the chemical structure of BBL, two potential initiation mechanisms for the ROP of BBL have been proposed (Scheme 2).[8,34] Path **a** is opened at the acyl−oxygen bond, generating polymers that are terminated by a hydroxyl group at one end and whose stereochemistry of the achiral center is undisturbed; path **b** is that the initiator, acting as a nucleophile (Nu), attacks the lactone ring splitting of C−O (alkyl−oxygen) bond, affording a carboxylate end-group and undergoing inversion of the chiral methine carbon after quenching with acid. However, the ^{1}H NMR spectrum and MALDI-TOF mass spectrum of the acid-quenched PHB samples catalyzed by complex **2** revealed that they possess a carboxylate group at one end and the other end group is a terminal hydroxyl group (Figures 2c and S11). This result precludes us from judging whether the

https://doi.org/10.1021/acs.macromol.4c02043
Macromolecules 2024, 57, 9275−9288

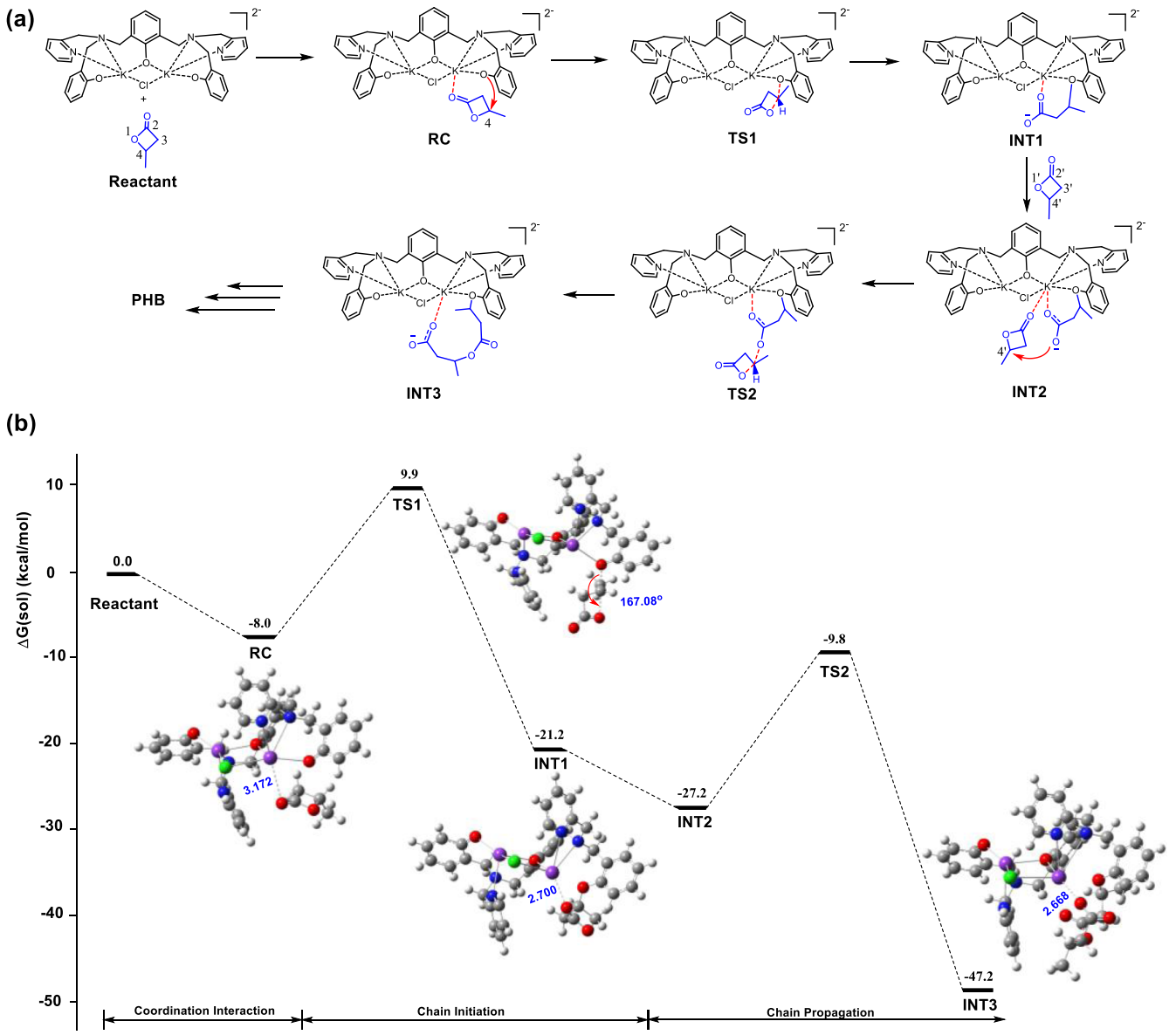

Figure 5. (a) Plausible mechanism for the ROP of BBL with complex **2** as a catalyst. (b) DFT-calculated free energy profiles at the B3LYP/6-31G (d, p) level and the optimized geometries of key intermediates and transition states for the ROP of BBL with complex **2**. The dashed lines depict binding interactions given in Angstrom.

ROP of BBL initiates in path **a** or **b**. To determine the route involved in the ROP of BBL with **2** even further, the polymerization reaction was conducted by **2** ($[(S)\text{-BBL}]_0/[\mathbf{2}]_0$ = 200, room temperature, 2 h, conversion = 83.2%), affording highly isotactic PHB, as demonstrated by ^{13}C NMR (Figure S29) with a T_m of 153 °C (Figure S30). Polarimetry at 365 nm revealed an $[\alpha]_{365}^{25}$ value of +3.2° (c = 0.011 g/mL), which is consistent with the polarimetry of (*R*)-PHB, demonstrating the inversion of the (*S*)-stereocenter.[33] These aforementioned observations clearly supported the cleavage of the alkyl−oxygen bond during the process of **2**-catalyzed ROP of BBL.

Due to the unexpected catalytic activity and good control over molecular weight distributions of **2**, we carried out DFT methods at the M06-2X/6-31 + G (d, p) level to simulate chain initiation and propagation processes, which proceed through the split of the alkyl−oxygen bond (path **b**), being aimed at better understanding the mechanism of **2**-mediated BBL polymerization. To reduce the time for the calculation work, a simple ligand without a substituted group was employed as a model ligand, and the tetra-alkyl ammonium group was omitted. The Gibbs free energy profiles determined for the ROP of BBL mediated by **2** are presented in Figure 5. According to the results of kinetic experiments, one molecular catalyst should be combined with two molecular monomers, and the two peripheral phenolate anions are initiated separately in the ROP of BBL. To decrease the computational workload, the calculation was performed with only one phenolate anion that initiated the ROP of BBL, and so did the mechanism diagram (Figure 5a).

The calculated reaction coordinate for the ring-opening of BBL involves the initial formation of a reactant complex (RC), which is 8.0 kcal mol^{-1} more stable than the reactants due to the weak coordination interaction between the potassium ion and the carbonyl oxygen of BBL (K···O = 3.172 Å). Subsequent nucleophilic attack of the phenolate anion on the C4 carbon atom of BBL proceeds via transition state TS1

https://doi.org/10.1021/acs.macromol.4c02043
Macromolecules 2024, 57, 9275−9288

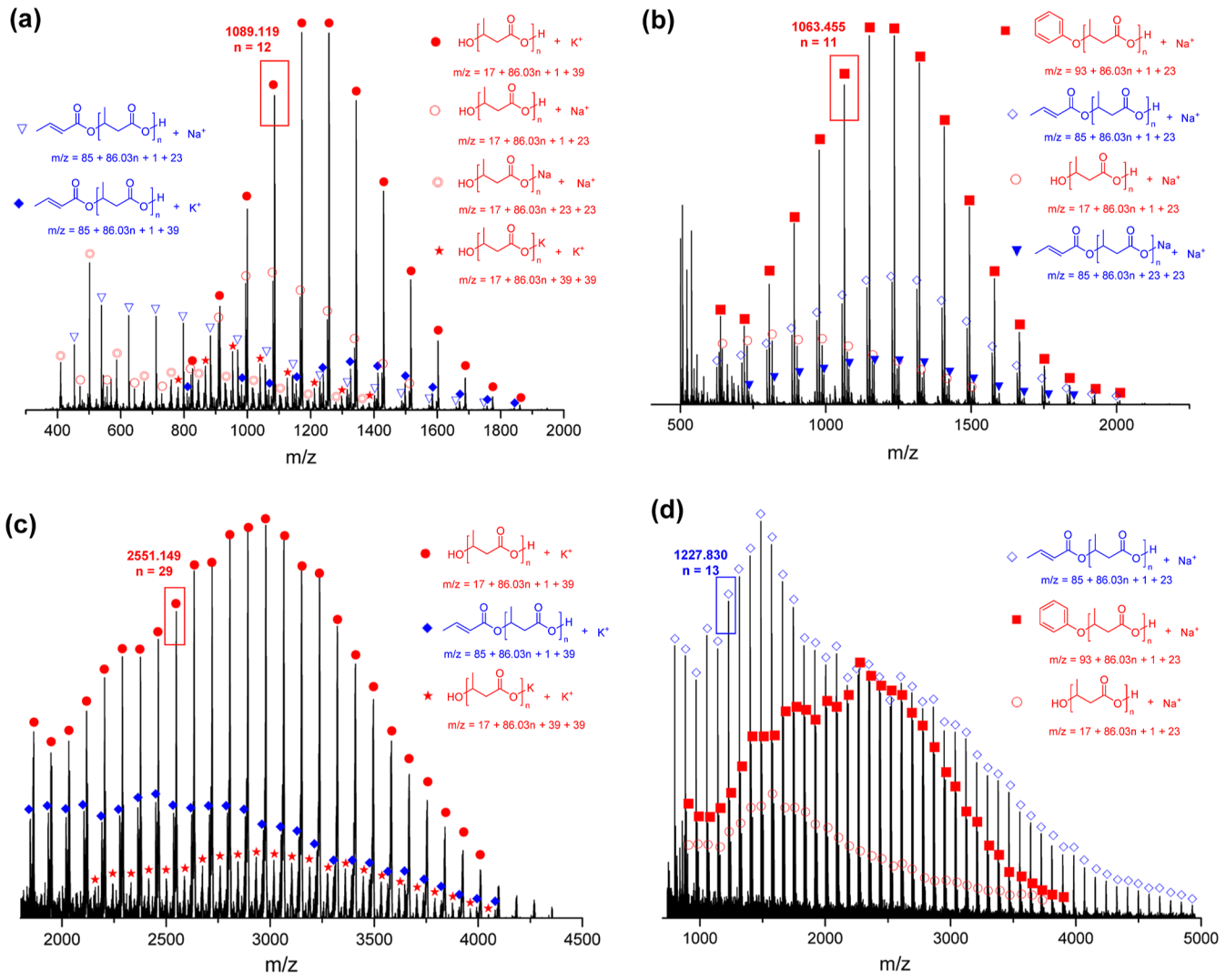

Figure 6. MALDI-TOF mass spectrum of PHBs (matrix: DHB; ionization salt: CF_3CO_2Na; solvent: THF): (a) $[rac\text{-BBL}]_0/[\mathbf{2}]_0$ = 200:1, 16% conversion, at room temperature in bulk; (b) $[rac\text{-BBL}]_0/[\mathbf{TBAPA}]_0$ = 100:1, 14% conversion, at room temperature in bulk; (c) $[rac\text{-BBL}]_0/[\mathbf{2}]_0$ = 200:1, 85% conversion, at room temperature in bulk; (d) $[rac\text{-BBL}]_0/[\mathbf{TBAPA}]_0$ = 100:1, 82% conversion, at room temperature in bulk.

with an activation barrier of 17.9 kcal mol^{-1}. The geometry of the TS1 is reminiscent of an S_N2-type one, in which the O−C−O angle is almost colinear (167.8°) (Figure 5b). The resulting carboxylate anion intermediate INT1 is stabilized via ion-pairing interactions (K···O = 2.700 Å). Chain propagation involves the combination of an additional BBL monomer to afford intermediate INT2. Then the reactive carboxylate anion reacts with a second molecule of BBL through the nucleophilic attack onto the C4′ atom to split the C_{alkyl}−O bond and give a pendant carboxylate unit, affording INT3 by overcoming an energy barrier of 17.4 kcal mol^{-1} (TS2). Conceivably, the above ring-opening process recursively repeats to afford chain growth of PHB until the quenching agent is added. Obviously, the larger Gibbs free energy drops for the nucleophilic attack of the phenolate anion (chain initiation) and the chain carboxylate anion end-group to monomer (chain propagation) were observed for **2**-involved initiator and propagation process (RC → INT1, −13.2 kcal mol^{-1}, and INT2 → INT3, −20.0 kcal mol^{-1}), in addition to the smaller energy barriers of the chain initiation (17.9 kcal mol^{-1}) and chain propagation (17.4 kcal mol^{-1}), indicating that the whole catalytic process of the ROP is very efficient not only in thermodynamics but also in kinetics, which guaranteed that the BBL polymerization would undergo in a fast fashion as we observed (Figure 5b; Table 1 entries 2−8).

Impact of the Ion-Pairing Interactions on Side Reaction. Intriguingly, we found that the strong ion-pairing interactions between the carboxylate anion of the growing chain end and K^+ are always observed in the geometry optimization process (INT1, K···O = 2.700 Å, and INT3, K···O = 2.668 Å) (Figure 5b). What role do these ion-pairing interactions play in the ROP of the BBL? To explore this problem, we synthesized tetrabutylammonium phenolate (**TBAPA**) (Figures S31 and S32) without metal ions as a catalyst for the ROP of BBL and carried out a series of control experiments. In the first place, the polymerizations were conducted at 16% conversion for $[rac\text{-BBL}]_0/[\mathbf{2}]_0$ = 200 and 14% conversion for $[rac\text{-BBL}]_0/[\mathbf{TBAPA}]_0$ = 100, respectively. By comparison with MALDI-TOF spectra (Figure 6a,b), we found that **2** or **TBAPA**-derived linear PHBs mainly include two categories: one is initiated with the nucleophilic phenolate anion for obtaining PHBs terminated phenoxy (phenyl ether) or hydroxyl group (from hydrolysis of phenyl ether) at one end and the carboxylate at the other end (marked in red); the other

https://doi.org/10.1021/acs.macromol.4c02043
Macromolecules 2024, 57, 9275−9288

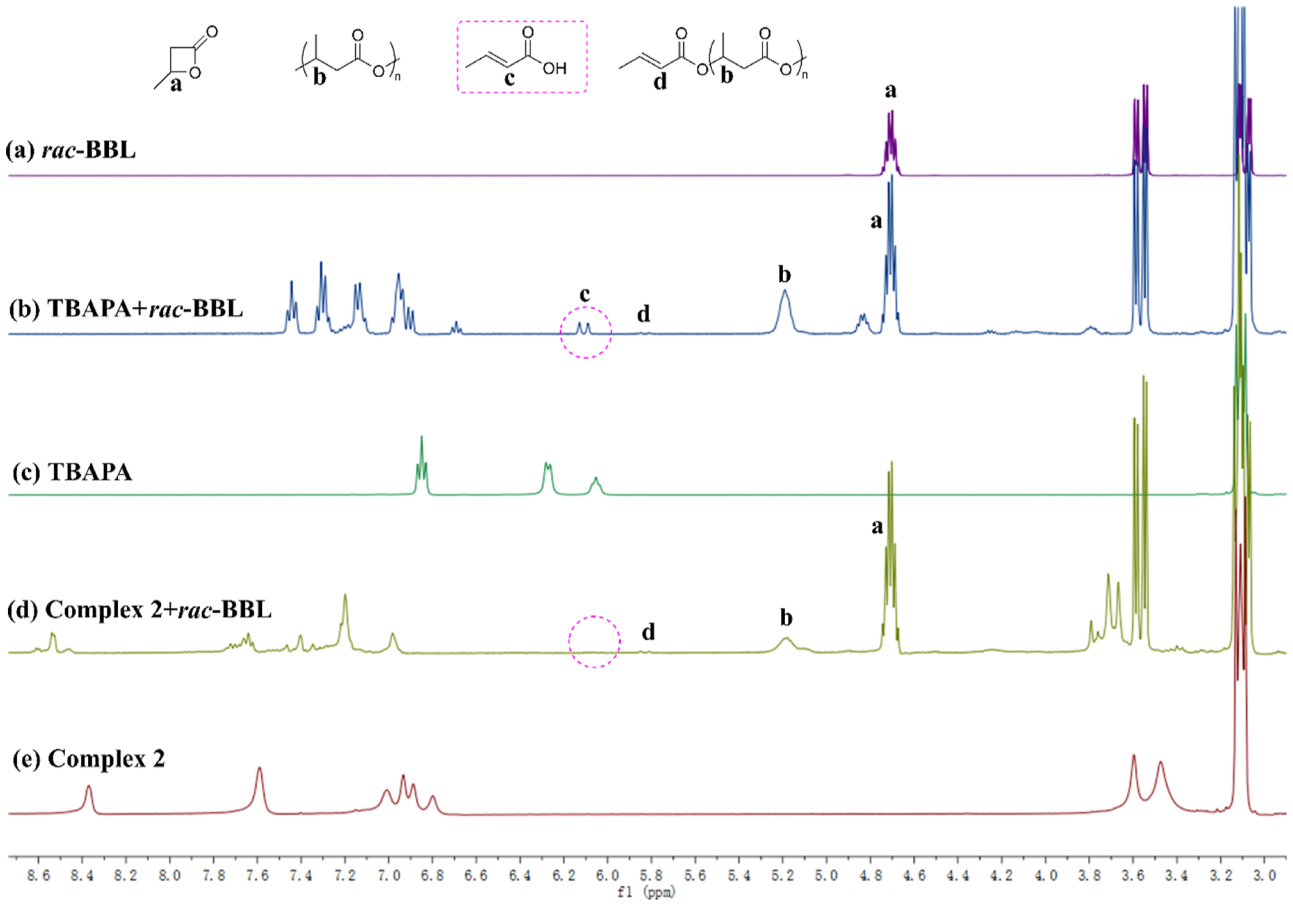

Figure 7. ^{1}H NMR spectra in dry CD_3CN-d_3 at 25 °C (a) *rac*-BBL; (b) $[rac\text{-BBL}]_0/[\mathbf{TBAPA}]_0$ = 10:1, $[\mathbf{TBAPA}]_0$ = 0.02 M, 12 h, at room temperature; (c) **TBAPA**; (d) $[rac\text{-BBL}]_0/[\text{complex } \mathbf{2}]_0$ = 20:1, $[\text{complex } \mathbf{2}]_0$ = 0.004 M, 12 h, at room temperature; and (e) complex **2**.

is PHBs containing the crotonate and carboxylate as the chain-end groups (marked in blue). At low conversions, the PHBs that are produced using **2** as a catalyst possess more narrow distributions and a lower ratio of crotonate-capped PHBs when compared with **TBAPA**. In addition, when *rac*-BBL was mixed with **2** at a ratio of 20:1 and **TBAPA** at a ratio of 10:1 in dry deuterated acetonitrile for about 12 h, respectively, the ^{1}H NMR spectra also revealed the fact that a good deal of the signals of crotonic acid species[33] formed after the based-promoted elimination reaction appeared in the **TBAPA**-catalyzed system and the corresponding peaks were hardly observed by **2** (Figure 7). These results meant that the phenolate anion in **2** has a weaker alkalinity than that in **TBAPA** due to the presence of the K^+ ion, which generates less crotonate active species by abstracting an acidic proton from the α-position of BBL in the initiation stage, resulting in a lower content of the crotonate-terminated PHBs. Subsequently, we carried out a theoretical calculation of the process of abstraction of an acidic proton when a phenolate anion of **2** serves as a base. Although the transition state of the proton transfer process is not found, the energy barrier of the cleavage of the alkyl−oxygen bond of BBL is 23.1 kcal mol^{-1}, which is higher than that of the ROP initiated by the nucleophilic phenolate anion (17.9 kcal mol^{-1}), illustrating that the deprotonation process would proceed more slowly.

With further analysis of the sample prepared at high conversions (85% for **2** and 82% for **TBAPA**) by MALDI-TOF, we found that the produced PHBs bearing the crotonate end-group derived from **2** as a catalyst have not increased significantly. In contrast, the polymers bearing the crotonate end-group for **TBAPA** as a catalyst have occupied a dominant position (Figure 6c,d). ^{1}H NMR spectra also confirmed that **TBAPA** could produce significantly more crotonate-terminated polymers than **2** (the content of the crotonate end-group is 4.12% for **TBAPA** with 83% conversion; the content of the crotonate end-group is 2.32% for **2** with 89% conversion) (Figures S33 and S34). Furthermore, the control experiment using tetrabutylammonium acetate (**TBAA**) as the metal-free catalyst for the ROP of *rac*-BBL was conducted within 2 h at room temperature in bulk with a 100:1 ratio of $[rac\text{-BBL}]_0/[\mathbf{TBAA}]_0$. ^{1}H NMR analysis showed that only 20% monomer conversion was reached and a lot of PHBs bearing the crotonate end-group were observed (Figures S35 and S36). The corresponding MALDI-TOF MS also confirmed that the crotonate-terminated PHBs dominated (Figure S37). These experimental results indicated that ion-pairing interactions between the carboxylate anion of the growing chain end and K^+ in **2** can effectively inhibit side reactions (the production of crotonate-terminated PHBs) during the chain propagation stage. Conceivably, the phenolate anion/the carboxylate anion of the growing chain end may serve as a Brønsted base to abstract randomly an acidic proton of BBL monomer in the **TBAPA**-catalyzed system without K^+, thereby producing more crotonate-terminated PHBs.

In addition, we also performed DFT calculations to investigate the **TBAPA**-catalyzed ROP process of BBL (see the computational details of Supporting Information). The energy barrier of the initiation stage and the energy barrier of

https://doi.org/10.1021/acs.macromol.4c02043
Macromolecules 2024, 57, 9275−9288

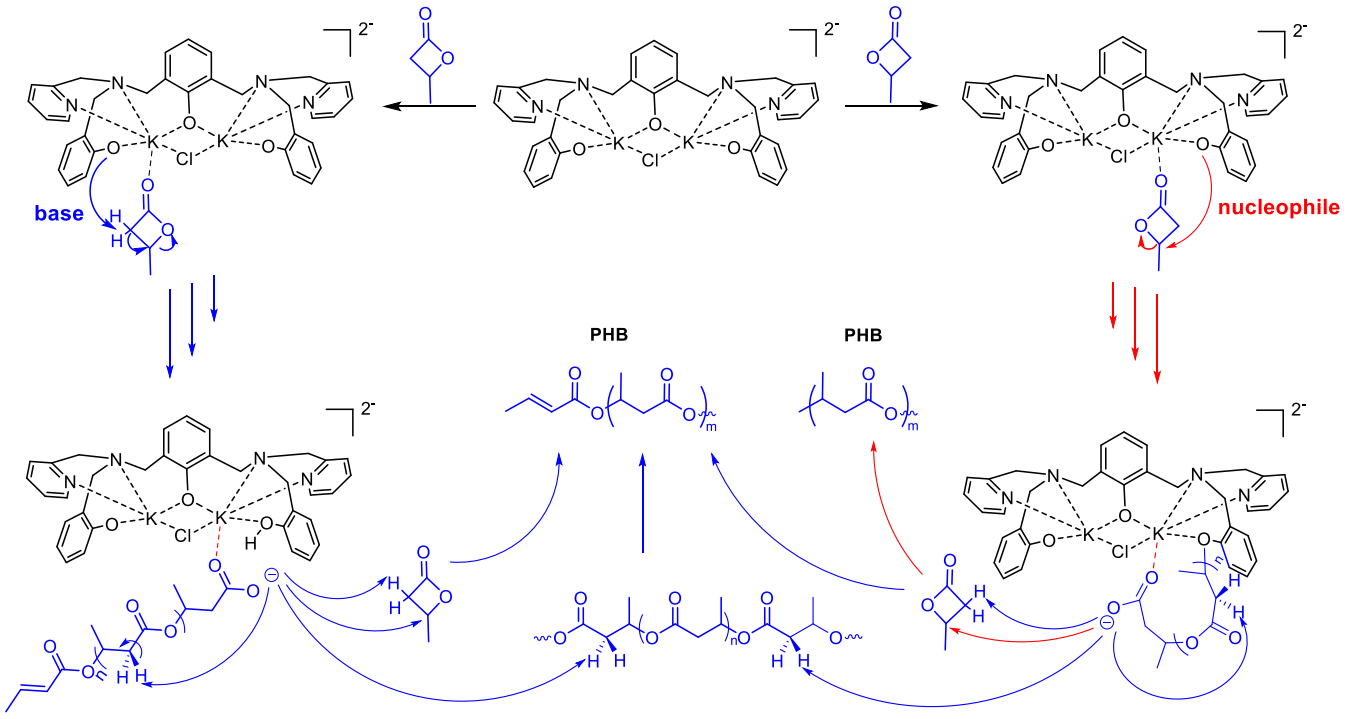

Figure 8. Possible mechanism for **2**-catalyzed the ROP of BBL. All substituted groups and tetrabutylammonium cations were omitted for clarity.

the chain propagation stage are 17.0 and 19.5 kcal mol^{-1}, respectively, indicating that chain propagation is the rate-determining step which is different from **2**. Due to the almost same energy barrier of chain initiation (17.4 kcal mol^{-1} for **2** vs 17.0 kcal mol^{-1} for **TBAPA**), the energy barrier of chain propagation stage (19.5 kcal mol^{-1}) is higher than that of **2** (17.4 kcal mol^{-1}), manifesting that **2** has higher catalytic activity compared to **TBAPA**, which is also in accordance with the experimental results (Table 1, entry 2 vs Table S3 entry 1).

In fact, the **2**-catalyzed ROP of BBL still contained a small amount of crotonate-terminated PHBs, which indicates that the existence of ion-pairing interactions cannot completely inhibit the production of PHBs bearing the crotonate end-group. From the above experimental results, it has been proven that these crotonate-terminated PHB can be produced by active species (phenolate anion or carboxylate anion) abstracting an acidic proton from the α-position of BBLmonomer. So, would these crotonate-terminated polymers be produced by the active carboxylate anion of the propagating chain abstracting an acidic proton from the growing chain itself or other polymer chains? To figure out this problem, a series of experiments were implemented, and the polymerizations were quenched at different conversions or different times ($[rac\text{-}BBL]_0/[\mathbf{2}]_0$ = 100:1, bulk, room temperature). When the monomer conversion increased from 66% to 91%, the content of the crotonate end-group slightly increased from 3.69% to 3.75% in the **2**-catalyzed system (Figures S38 and S39). However, when all the monomers were exhausted and the reaction continued for half an hour, the content of the crotonate end-group was significantly increased to 4.34% (Figure S40). The above experiments showed that a small amount of crotonate-terminated PHBs can be produced not only by active species (phenolate anion or carboxylate anion) abstracting an acidic proton from the BBL monomer but also by the active carboxylate anion of the propagating chain abstracting an acidic proton from the growing chain itself or other polymer chains in the **2**-catalyzed ROP of BBL.

Proposed Mechanism and Possible Side Reactions in the 2-Mediated ROP of BBL. By integrating all of these experimental and theoretically calculated facts, we proposed a possible mechanism for **2**-catalyzed ROP of BBL (Figure 8). The phenolate anion of **2** can act not only as a nucleophile to attack the BBL ring splitting of the C−O (alkyl−oxygen) bond for generating an active carboxylate species but also as a base to extract an acidic proton from the α-position of BBL to generate a crotonate active species. On the one hand, these two active species containing the carboxylate as an end-group can serve as a new nucleophile to open the BBL ring for chain growth by breaking the alkyl−oxygen bond to enchain BBL. On the other hand, both the carboxylate end of these active species can also be used as a base to promote the elimination of the growing chain itself or other chains. Due to the presence of K^+, the alkalinity of phenolate anion in **2** is less, so the speed of abstraction of an acidic proton of BBL in **2** is relatively slow, which partially inhibits the side reaction in the initiation stage. Moreover, in the chain propagation stage, the ion-pairing interactions between the K^+ and the active terminal carboxylate can inhibit the random abstraction of an acidic proton from the monomer and the growing chain itself or other polymer chains, which facilitates the polymerization more controllable and obtain high molecular weight PHB. With the increase of the polymerization degree, the ion-pairing interactions between the K^+ ion and terminal carboxylate group may be gradually weakened due to the formation of a larger macrocycle during propagation. The occurrence of this phenomenon will lead to the inhibitory effect on side reactions that may be weakened so that this system cannot gain ultrahigh molecular weight PHB (>100 kg mol^{-1}).

https://doi.org/10.1021/acs.macromol.4c02043
Macromolecules 2024, 57, 9275−9288

CONCLUSIONS

In summary, we developed a novel series of dinuclear sodium- and potassium ion-pair catalysts, which can effectively promote the rapid and controlled ROP of BBL at room temperature. Systematical investigations were carried out, and it was found that the ion-pairing interactions between the bulky $N^nBu_4^+$ and $[K_2(\mu_2\text{-}L_1)(\mu_2\text{-}Cl)]^{2-}$/carboxylate anion can weaken the binding interactions originating from the phenolate anion/propagating carboxylate anion and the K^+ ion, thus enhancing the nucleophilicity of the initiator (phenolate anion) and chain end (carboxylate anion) for accelerating the polymerization rate; on the other hand, the ion-pairing interactions between K^+ ions and phenolate anion/the propagating carboxylate anion decrease the corresponding anionic alkalinity for inhibiting the side reaction. In addition, these dinuclear sodium and potassium ion-pair catalysts were innocuous, low-cost, easily synthesized, and coupled with high catalytic activity, and had good control on the ROP, implying their potential for the low cost of producing PHB. Collectively, this strategy not only offers a new approach to designing sodium and potassium-based catalysts for the efficient ROP of BBL but also broadens the application scope of ion-pairing interactions in the field of catalysis. Future work will focus on the asymmetric induction originating from chiral ion-pairing complexes for stereoselective *rac*-BBL polymerization to prepare PHB with excellent properties.

ASSOCIATED CONTENT

Supporting Information

The Supporting Information is available free of charge at https://pubs.acs.org/doi/10.1021/acs.macromol.4c02043.

Experimental details and characterization of ligands H_3L_1-H_3L_4, **TBAPA**, and complexes **1**−**7** (PDF)

X-ray crystallographic data of complex **1′** with CCDC reference number of 2347440 (CIF)

X-ray crystallographic data of complex **2″** with CCDC reference number of 2360354 (CIF)

X-ray crystallographic data of complex **1** with CCDC reference number of 2347403 (CIF)

X-ray crystal structure data for complex **1′** and the polymerization studies and computational details (PDF)

X-ray crystal structure data for complex **2″** and the polymerization studies and computational details (PDF)

X-ray crystal structure data for complex **1** and the polymerization studies and computational details (PDF)

AUTHOR INFORMATION

Corresponding Author

Aijiang Zhang − *College of Chemistry and Pharmaceutical Engineering, Huanghuai University, Zhumadian 463000, People's Republic of China;* orcid.org/0000-0002-1870-4431; Email: 20111205@huanghuai.edu.cn

Authors

Changjuan Chen − *College of Chemistry and Pharmaceutical Engineering, Huanghuai University, Zhumadian 463000, People's Republic of China;* orcid.org/0000-0002-2388-6559

Chunshan Zuo − *College of Chemistry and Pharmaceutical Engineering, Huanghuai University, Zhumadian 463000, People's Republic of China*

Jianghong Dong − *College of Chemistry and Pharmaceutical Engineering, Huanghuai University, Zhumadian 463000, People's Republic of China;* orcid.org/0000-0002-3008-3594

Mingjian Ma − *College of Chemistry and Pharmaceutical Engineering, Huanghuai University, Zhumadian 463000, People's Republic of China*

Shihao Zhang − *College of Chemistry and Pharmaceutical Engineering, Huanghuai University, Zhumadian 463000, People's Republic of China*

Huyuan Guo − *College of Chemistry and Pharmaceutical Engineering, Huanghuai University, Zhumadian 463000, People's Republic of China*

Jing Fu − *College of Chemistry and Pharmaceutical Engineering, Huanghuai University, Zhumadian 463000, People's Republic of China*

Complete contact information is available at: https://pubs.acs.org/10.1021/acs.macromol.4c02043

Notes

The authors declare no competing financial interest.

ACKNOWLEDGMENTS

We acknowledge the financial support from the National Natural Science Foundation of China (21901082 and 21301064), the Programs for Science and Technology Department of Henan Province (192102210023 and 242102310440), and the Cultivation Project of Huanghuai University (XKPY-2022021).

REFERENCES

(1) Jambeck, J. R.; Geyer, R.; Wilcox, C.; Siegler, T. R.; Perryman, M.; Andrady, A.; Narayan, R.; Law, K. L. Plastic Waste Inputs from Land into the Ocean. *Science* **2015**, *347*, 768−771.

(2) MacLeod, M.; Arp, H. P. H.; Tekman, M. B.; Jahnke, A. The Global Threat from Plastic Pollution. *Science* **2021**, *373*, 61−65.

(3) Zhu, Y.; Romain, C.; Williams, C. K. Sustainable Polymers from Renewable Resources. *Nature* **2016**, *540*, 354−362.

(4) Zhang, X.; Fevre, M.; Jones, G. O.; Waymouth, R. M. Catalysis as an Enabling Science for Sustainable Polymers. *Chem. Rev.* **2018**, *118*, 839−885.

(5) Haque, F. M.; Ishibashi, J. S. A.; Lidston, C. A. L.; Shao, H.; Bates, F. S.; Chang, A. B.; Coates, G. W.; Cramer, C. J.; Dauenhauer, P. J.; Dichtel, W. R.; Ellison, C. J.; Gormong, E. A.; Hamachi, L. S.; Hoye, T. R.; Jin, M.; Kalow, J. A.; Kim, H. J.; Kumar, G.; LaSalle, C. J.; Liffland, S.; Lipinski, B. M.; Pang, Y.; Parveen, R.; Peng, X.; Popowski, Y.; Prebihalo, E. A.; Reddi, Y.; Reineke, T. M.; Sheppard, D. T.; Swartz, J. L.; Tolman, W. B.; Vlaisavljevich, B.; Wissinger, J.; Xu, S.; Hillmyer, M. A. Defining the Macromolecules of Tomorrow through Synergistic Sustainable Polymer Research. *Chem. Rev.* **2022**, *122*, 6322−6373.

(6) Khalil, A.; Cammas-Marion, S.; Coulembier, O. Organocatalysis applied to the ring-opening polymerization of β-lactones: A brief overview. *J. Polym. Sci., Part A: Polym. Chem.* **2019**, *57*, 657−672.

(7) Chen, G.-Q. A Microbial Polyhydroxyalkanoates (PHA) Based Bio- and Materials Industry. *Chem. Soc. Rev.* **2009**, *38*, 2434−2446.

(8) Rieth, L. R.; Moore, D. R.; Lobkovsky, E. B.; Coates, G. W. Single-Site β-Diiminate Zinc Catalysts for the Ring-Opening Polymerization of β-Butyrolactone and β-Valerolactone to Poly(3-hydroxyalkanoates). *J. Am. Chem. Soc.* **2002**, *124*, 15239−15248.

(9) Yang, J.-C.; Yang, J.; Li, W.-B.; Lu, X.-B.; Liu, Y. Carbonylative Polymerization of Epoxides Mediated by Tri-metallic Complexes: A Dual Catalysis Strategy for Synthesis of Biodegradable Polyhydroxyalkanoates. *Angew. Chem., Int. Ed.* **2022**, *61*, No. e202116208.

(10) Brulé, E.; Gaillard, S.; Rager, M.-N.; Roisnel, T.; Guérineau, V.; Nolan, S. P.; Thomas, C. M. Polymerization of Racemic β-Butyrolactone Using Gold Catalysts: A Simple Access to Biodegradable Polymers. *Organometallics* **2011**, *30*, 2650−2653.
(11) Wang, H.; Guo, J.; Yang, Y.; Ma, H. Diastereoselective Synthesis of Chiral Aminophenolate Magnesium Complexes and their Application in the Stereoselective Polymerization of *rac*-Lactide and *rac*-β-Butyrolactone. *Dalton Trans.* **2016**, *45*, 10942−10953.
(12) Westlie, A. H.; Quinn, E. C.; Parker, C. R.; Chen, E. Y. X. Synthetic Biodegradable Polyhydroxyalkanoates (PHAs): Recent Advances and Future Challenges. *Prog. Polym. Sci.* **2022**, *134*, 101608.
(13) Amgoune, A.; Thomas, C. M.; Ilinca, S.; Roisnel, T.; Carpentier, J.-F. Highly Active, Productive, and Syndiospecific Yttrium Initiators for the Polymerization of Racemic β-Butyrolactone. *Angew. Chem., Int. Ed.* **2006**, *45*, 2782−2784.
(14) Ligny, R.; Hänninen, M. M.; Guillaume, S. M.; Carpentier, J.-F. Steric vs. Electronic Stereocontrol in Syndio- or Iso-Selective ROP of Functional Chiral β-Lactones Mediated by Achiral Yttrium-Bisphenolate Complexes. *Chem. Commun.* **2018**, *54*, 8024−8031.
(15) Zhuo, Z.; Zhang, C.; Luo, Y.; Wang, Y.; Yao, Y.; Yuan, D.; Cui, D. Stereo-Selectivity Switchable ROP of *rac*-β-Butyrolactone Initiated by Salan-Ligated Rare-Earth Metal Amide Complexes: The Key Role of the Substituents on Ligand Frameworks. *Chem. Commun.* **2018**, *54*, 11998−12001.
(16) Liu, H.; Shi, X. Phosphasalalen Rare-Earth Complexes for the Polymerization of *rac*-Lactide and *rac*-β-Butyrolactone. *Inorg. Chem.* **2021**, *60*, 705−717.
(17) Dong, X.; Brown, A. M.; Woodside, A. J.; Robinson, J. R. N-Oxides Amplify Catalyst Reactivity and Isoselectivity in the Ring-Opening Polymerization of *rac*-β-Butyrolactone. *Chem. Commun.* **2022**, *58*, 2854−2857.
(18) Bruckmoser, J.; Pongratz, S.; Stieglitz, L.; Rieger, B. Highly Isoselective Ring-Opening Polymerization of *rac*-β-Butyrolactone: Access to Synthetic Poly(3-hydroxybutyrate) with Polyolefin-like Material Properties. *J. Am. Chem. Soc.* **2023**, *145*, 11494−11498.
(19) Huang, H.-Y.; Xiong, W.; Huang, Y.-T.; Li, K.; Cai, Z.; Zhu, J.-B. Spiro-Salen Catalysts Enable the Chemical Synthesis of Stereoregular Polyhydroxyalkanoates. *Nat. Catal.* **2023**, *6*, 720−728.
(20) Zintl, M.; Molnar, F.; Urban, T.; Bernhart, V.; Preishuber-Pflügl, P.; Rieger, B. Variably Isotactic Poly(hydroxybutyrate) from Racemic β-Butyrolactone: Microstructure Control by Achiral Chromium(III) Salophen Complexes. *Angew. Chem., Int. Ed.* **2008**, *47*, 3458−3460.
(21) Reichardt, R.; Vagin, S.; Reithmeier, R.; Ott, A. K.; Rieger, B. Factors Influencing the Ring-Opening Polymerization of Racemic β-Butyrolactone Using Cr^{III}(salphen). *Macromolecules* **2010**, *43*, 9311−9317.
(22) Jeffery, B. J.; Whitelaw, E. L.; Garcia-Vivo, D.; Stewart, J. A.; Mahon, M. F.; Davidson, M. G.; Jones, M. D. Group 4 Initiators for the Stereoselective ROP of rac-β-Butyrolactone and its Copolymerization with rac-Lactide. *Chem. Commun.* **2011**, *47*, 12328−12330.
(23) Luciano, E.; Buonerba, A.; Grassi, A.; Milione, S.; Capacchione, C. Thioetherphenolate Group 4 Metal Complexes in the Ring Opening Polymerization of *rac*-β-Butyrolactone. *J. Polym. Sci., Part A: Polym. Chem.* **2016**, *54*, 3132−3139.
(24) Ebrahimi, T.; Aluthge, D. C.; Hatzikiriakos, S. G.; Mehrkhodavandi, P. Highly Active Chiral Zinc Catalysts for Immortal Polymerization of β-Butyrolactone Form Melt Processable Syndio-Rich Poly(hydroxybutyrate). *Macromolecules* **2016**, *49*, 8812−8824.
(25) Shaik, M.; Peterson, J.; Du, G. Cyclic and Linear Polyhydroxylbutyrates from Ring-Opening Polymerization of β-Butyrolactone with Amido-Oxazolinate Zinc Catalysts. *Macromolecules* **2019**, *52*, 157−166.
(26) Gruszka, W.; Walker, L. C.; Shaver, M. P.; Garden, J. A. In Situ Versus Isolated Zinc Catalysts in the Selective Synthesis of Homo and Multi-block Polyesters. *Macromolecules* **2020**, *53*, 4294−4302.
(27) Cross, E. D.; Allan, L. E. N.; Decken, A.; Shaver, M. P. Aluminum Salen and Salan Complexes in the Ring-Opening Polymerization of Cyclic Esters: Controlled Immortal and Copolymerization of *rac*-β-Butyrolactone and rac-Lactide. *J. Polym. Sci., Part A: Polym. Chem.* **2013**, *51*, 1137−1146.
(28) García-Valle, F. M.; Tabernero, V.; Cuenca, T.; Mosquera, M. E. G.; Cano, J.; Milione, S. Biodegradable PHB from *rac*-β-Butyrolactone: Highly Controlled ROP Mediated by a Pentacoordinated Aluminum Complex. *Organometallics* **2018**, *37*, 837−840.
(29) Ebrahimi, T.; Hatzikiriakos, S. G.; Mehrkhodavandi, P. Synthesis and Rheological Characterization of Star-Shaped and Linear Poly(hydroxybutyrate). *Macromolecules* **2015**, *48*, 6672−6681.
(30) Yuntawattana, N.; McGuire, T. M.; Durr, C. B.; Buchard, A.; Williams, C. K. Indium Phosphasalen Catalysts Showing High Isoselectivity and Activity in Racemic Lactide and Lactone Ring Opening Polymerizations. *Catal. Sci. Technol.* **2020**, *10*, 7226−7239.
(31) Bruckmoser, J.; Henschel, D.; Vagin, S.; Rieger, B. Combining High Activity with Broad Monomer Scope: Indium Salan Catalysts in the Ring-Opening Polymerization of Various Cyclic Esters. *Catal. Sci. Technol.* **2022**, *12*, 3295−3302.
(32) Kricheldorf, H. R.; Eggerstedt, S. Polylactones. 41. Polymerizations of β-d,l-Butyrolactone with Dialkyltinoxides as Initiators. *Macromolecules* **1997**, *30*, 5693−5697.
(33) Yang, L.; Zhang, Y.-Y.; Yang, G.-W.; Xie, R.; Wu, G.-P. Controlled Ring-Opening Polymerization of β-Butyrolactone Via Bifunctional Organoboron Catalysts. *Macromolecules* **2021**, *54*, 5509−5517.
(34) Sánchez-Roa, D.; Sessini, V.; Mosquera, M. E. G.; Cámpora, J. N-Heterocyclic Carbene-Carbodiimide (NHC-CDI) Betaines as Organocatalysts for β-Butyrolactone Polymerization: Synthesis of Green PHB Plasticizers with Tailored Molecular Weights. *ACS Catal.* **2024**, *14*, 2487−2501.
(35) Devaine-Pressing, K.; Oldenburg, F. J.; Menzel, J. P.; Springer, M.; Dawe, L. N.; Kozak, C. M. Lithium, Sodium, Potassium and Calcium Amine-bis(phenolate) Complexes in the Ring-Opening Polymerization of *rac*-Lactide. *Dalton Trans.* **2020**, *49*, 1531−1544.
(36) Gao, J.; Zhu, D.; Zhang, W.; Solan, G. A.; Ma, Y.; Sun, W.-H. Recent Progress in the Application of Group 1, 2 & 13 Metal Complexes as Catalysts for the Ring Opening Polymerization of Cyclic Esters. *Inorg. Chem. Front.* **2019**, *6*, 2619−2652.
(37) Gentner, T. X.; Mulvey, R. E. Alkali-Metal Mediation: Diversity of Applications in Main-Group Organometallic Chemistry. *Angew. Chem., Int. Ed.* **2021**, *60*, 9247−9262.
(38) Xu, C.; Yu, I.; Mehrkhodavandi, P. Highly controlled immortal polymerization of β-butyrolactone by a dinuclear indium catalyst. *Chem. Commun.* **2012**, *48*, 6806−6808.
(39) Dong, X.; Robinson, J. R. The Role of Neutral Donor Ligands in the Isoselective Ring-Opening Polymerization of *rac*-β-Butyrolactone. *Chem. Sci.* **2020**, *11*, 8184−8195.
(40) Juzwa, M.; Jedliński, Z. Novel Synthesis of Poly(3-hydroxybutyrate). *Macromolecules* **2006**, *39*, 4627−4630.
(41) Kawalec, M.; Śmiga-Matuszowicz, M.; Kurcok, P. Counterion and Solvent Effects on the Anionic Polymerization of β-Butyrolactone Initiated with Acetic Acid Salts. *Eur. Polym. J.* **2008**, *44*, 3556−3563.
(42) Adamus, G.; Kowalczuk, M. Anionic Ring-Opening Polymerization of β-Alkoxymethyl-Substituted β-Lactones. *Biomacromolecules* **2008**, *9*, 696−703.
(43) Jedliński, Z.; Kowalczuk, M.; Kurcok, P.; Adamus, G.; Matuszowicz, A.; Sikorska, W.; Gross, R. A.; Xu, J.; Lenz, R. W. Stereochemical Control in the Anionic Polymerization of β-Butyrolactone Initiated with Alkali-Metal Alkoxides. *Macromolecules* **1996**, *29*, 3773−3777.
(44) Brak, K.; Jacobsen, E. N. Asymmetric Ion-Pairing Catalysis. *Angew. Chem., Int. Ed.* **2013**, *52*, 534−561.
(45) Qian, D.; Sun, J. Recent Progress in Asymmetric Ion-Pairing Catalysis with Ammonium Salts. *Chem.—Eur. J.* **2019**, *25*, 3740−3751.
(46) Uraguchi, D.; Kimura, Y.; Ueoka, F.; Ooi, T. Urea as a Redox-Active Directing Group under Asymmetric Photocatalysis of Iridium-Chiral Borate Ion Pairs. *J. Am. Chem. Soc.* **2020**, *142*, 19462−19467.
(47) Yang, X.; Gitter, S. R.; Roessler, A. G.; Zimmerman, P. M.; Boydston, A. J. An Ion-Pairing Approach to Stereoselective Metal-

https://doi.org/10.1021/acs.macromol.4c02043
Macromolecules 2024, 57, 9275−9288

Free Ring-Opening Metathesis Polymerization. *Angew. Chem., Int. Ed.* **2021**, *60*, 13952−13958.
(48) Gillespie, J. E.; Fanourakis, A.; Phipps, R. J. Strategies That Utilize Ion Pairing Interactions to Exert Selectivity Control in the Functionalization of C−H Bonds. *J. Am. Chem. Soc.* **2022**, *144*, 18195−18211.
(49) Schirmer, T. E.; König, B. Ion-Pairing Catalysis in Stereoselective, Light-Induced Transformations. *J. Am. Chem. Soc.* **2022**, *144*, 19207−19218.
(50) Yang, Z.; Xu, C.; Zhou, X.; Cheong, C. B.; Kee, C. W.; Tan, C.-H. A Chiral Pentanidium and Pyridinyl-Sulphonamide Ion Pair as an Enantioselective Organocatalyst for Steglich Rearrangement. *Chem. Sci.* **2023**, *14*, 13184−13190.
(51) Sorensen, C. C.; Kozuszek, C. T.; Borden, M. A.; Leibfarth, F. A. Asymmetric Ion-Pairing in Stereoselective Vinyl Polymerization. *ACS Catal.* **2023**, *13*, 3272−3284.
(52) Iribarren, I.; Mates-Torres, E.; Trujillo, C. Revisiting Ion-Pair Interactions in Phase Transfer Catalysis: from Ionic Compounds to Real Catalyst Systems. *Dalton Trans.* **2024**, *53*, 1322−1335.
(53) Yang, Z.; Liao, Y.; Zhang, Z.; Chen, J.; Zhang, X.; Liao, S. Asymmetric Ion-Pairing Photoredox Catalysis for Stereoselective Cationic Polymerization under Light Control. *J. Am. Chem. Soc.* **2024**, *146*, 6449−6455.
(54) Addison, A. W.; Rao, T. N.; Reedijk, J.; van Rijn, J.; Verschoor, G. C. Synthesis, Structure, and Spectroscopic Properties of Copper(II) Compounds Containing Nitrogen-Sulphur Donor Ligands; the Crystal and Molecular Structure of Aqua[1,7-bis(N-methylbenzimidazol-2'-yl)-2,6-dithiaheptane]copper(II) Perchlorate. *J. Chem. Soc., Dalton Trans.* **1984**, 1349−1356.
(55) Domiński, A.; Konieczny, T.; Zięba, M.; Klim, M.; Kurcok, P. Anionic Polymerization of β-Butyrolactone Initiated with Sodium Phenoxides. The Effect of the Initiator Basicity/Nucleophilicity on the ROP Mechanism. *Polymers* **2019**, *11*, 1221.
(56) Wu, Y.; Chen, K.; Wu, X.; Liu, L.; Zhang, W.; Ding, Y.; Liu, S.; Zhou, M.; Shao, N.; Ji, Z.; Chen, J.; Zhu, M.; Liu, R. Superfast and Water-Insensitive Polymerization on α-Amino Acid *N*-Carboxyanhydrides to Prepare Polypeptides Using Tetraalkylammonium Carboxylate as the Initiator. *Angew. Chem., Int. Ed.* **2021**, *60*, 26063−26071.

https://doi.org/10.1021/acs.macromol.4c02043
Macromolecules 2024, 57, 9275−9288